Negative longitudinal magnetoresistance in Dirac and Weyl metals

A. A. Burkov
Department of Physics and Astronomy, University of Waterloo, Waterloo, Ontario N2L 3G1, Canada
and National Research University ITMO, Saint Petersburg 197101, Russia
(Received 11 May 2015; published 29 June 2015)

It has recently been found that Dirac and Weyl metals are characterized by an unusual weak-field longitudinal magnetoresistance: large, negative, and quadratic in the magnetic field. This has been shown to arise from the chiral anomaly, i.e., nonconservation of the chiral charge in the presence of external electric and magnetic fields, oriented collinearly. In this paper we report on a theory of this effect in both Dirac and Weyl metals. We demonstrate that this phenomenon contains two important ingredients. One is the magnetic-field-induced coupling between the chiral and the total (or vector, in relativistic field theory terminology) charge densities. This arises from the Berry curvature and is present in principle whenever the Berry curvature is nonzero, i.e., is nonspecific to Dirac and Weyl metals. This coupling, however, leads to a large negative quadratic magnetoresistance only when the second ingredient is present, namely when the chiral charge density is a nearly conserved quantity with a long relaxation time. This property is specific to Dirac and Weyl metals and is realized only when the Fermi energy is close to Dirac or Weyl nodes, expressing an important low-energy property of these materials, emergent chiral symmetry.

DOI: 10.1103/PhysRevB.91.245157 PACS number(s): 75.47.−m, 03.65.Vf, 71.90.+q, 73.43.−f

I. INTRODUCTION

Weyl and closely related Dirac semimetals are the most recent addition to the growing family of materials with topologically nontrivial electronic structure. Both were initially predicted theoretically [1–9] and realized very recently in a remarkable series of experiments [10–23]. What distinguishes Weyl semimetals from other topologically nontrivial states of matter, such as topological insulators (TIs) [24,25], is that they are gapless. The topological object in this case is a point of contact between two nondegenerate bands at the Fermi level, which acts as a monopole source of Berry curvature and thus carries an integer topological charge. The significance of such electronic structure features was emphasized in earlier pioneering work of Volovik [26,27], which partly anticipated the recent developments.

A hallmark of "topological" states of matter is the presence of metallic edge states, which arise necessarily due to the impossibility of a smooth connection between the topologically nontrivial sample and its topologically trivial environment. A Weyl semimetal does indeed possess such surface states, whose topologically nontrivial nature is manifest in the shape of their Fermi surface, having the form of an open arc (Fermi arc), rather than a closed curve, as in any regular two-dimensional (2D) metal. These have been seen directly using ARPES in the newly discovered Weyl semimetal materials TaAs and NbAs [10–12,20].

However, topologically nontrivial phases of matter often also have unusual electromagnetic response, the most famous example being the precisely quantized transverse conductivity of a 2D quantum Hall liquid. Such a response is a robust, detail-independent manifestation of the nontrivial electronic structure topology on macroscopic scales and is thus of particular interest.

Topological electromagnetic response may be conveniently expressed as a topological term, generated in the action of the electromagnetic field, when electrons in the occupied states are integrated out. In the case of the 2D quantum Hall liquid, this is the Chern-Simons term

$$S = -\frac{e^2}{4\pi}\int dt\, d^2r\, \epsilon^{\nu\alpha\beta} A_\nu \partial_\alpha A_\beta, \tag{1}$$

where (and henceforth) $\hbar = c = 1$ units are used, and filling factor 1 is taken above for concreteness. This may be generalized to 3D by stacking the 2D quantum Hall systems along a particular spatial direction [28], which gives

$$S = -\frac{e^2}{8\pi^2}\int dt\, d^3r\, G_\mu \epsilon^{\mu\nu\alpha\beta} A_\nu \partial_\alpha A_\beta, \tag{2}$$

where $\mathbf{G} = 2\pi\hat{n}/d$ is a reciprocal lattice vector in the stacking direction $\hat{n}$, corresponding to superlattice period d. Using integration by parts, Eq. (2) may be rewritten in the following form, which will prove useful below:

$$S = \frac{e^2}{32\pi^2}\int dt\, d^3r\, \theta(\mathbf{r})\, \epsilon^{\mu\nu\alpha\beta} F_{\mu\nu} F_{\alpha\beta}, \tag{3}$$

where $\theta(\mathbf{r}) = \mathbf{G}\cdot\mathbf{r}$.

For a 3D TI, the topological term takes the form of the so-called θ term [25]

$$S = \frac{e^2}{32\pi^2}\int dt\, d^3r\, \theta\, \epsilon^{\mu\nu\alpha\beta} F_{\mu\nu} F_{\alpha\beta}, \tag{4}$$

where $\theta = \pi$ for a TI and $\theta = 0$ for a normal insulator (NI). Applying integration by parts as above, it is clear that Eq. (4) in fact has no observable consequences in the bulk of the TI, since it is a total derivative and vanishes upon integration by parts. It does have an effect on the TI boundaries: upon breaking time-reversal (TR) symmetry by, e.g., magnetic impurity doping, it leads to the half-quantized anomalous Hall effect (AHE) [24,25].

A Weyl semimetal may be regarded as an intermediate phase between a 3D TI (or NI) and the 3D quantum Hall insulator, described by Eq. (3) [3]. The topological term of a Weyl semimetal takes the form of Eq. (3), but with the field θ

 ©2015 American Physical Society

given by [29,30]

$$\theta(\mathbf{r},t) = 2\mathbf{b}\cdot\mathbf{r} - 2b_0 t, \tag{5}$$

where

$$\mathbf{b} = \frac{1}{2}\sum_i C_i \mathbf{K}_i,\ b_0 = \frac{1}{2}\sum_i C_i \epsilon_i. \tag{6}$$

Here C_i is the topological charge of the ith Weyl node, $\mathbf{K}_i$ is its location in momentum space, and ϵ_i is its energy. This is similar to topological terms arising in the context of Lorentz-invariance-violating extensions of the standard model of particle physics [31]. As is easy to see, the linear space-time coordinate dependence of the $\theta(\mathbf{r},t)$ field is the only nontrivial dependence compatible with space-time translational symmetry. Due to this space-time coordinate dependence, the topological term in Weyl semimetals does not vanish upon integration by parts, but instead takes the form, similar to Eq. (2),

$$S = -\frac{e^2}{8\pi^2}\int dt\, d^3r\, \partial_\mu\, \theta(\mathbf{r},t)\epsilon^{\mu\nu\alpha\beta} A_\nu \partial_\alpha A_\beta. \tag{7}$$

This, in turn, leads to a nontrivial modification of the Maxwell equations in the bulk of the Weyl semimetal, which may be expressed as two extra contributions to the current density, obtained by varying Eq. (7) with respect to the electromagnetic gauge potential

$$j_\nu = \frac{e^2}{2\pi^2} b_\mu \epsilon^{\mu\nu\alpha\beta}\partial_\alpha A_\beta, \quad \mu = 1,2,3, \tag{8}$$

and

$$j_\nu = -\frac{e^2}{2\pi^2} b_0 \epsilon^{0\nu\alpha\beta}\partial_\alpha A_\beta. \tag{9}$$

Equation (8) describes AHE with semiquantized Hall conductivity, proportional to the magnitude of the vector **b**, giving the separation between the Weyl nodes in momentum space, while Eq. (9) describes the so-called chiral magnetic effect (CME) [32]. We will return to the meaning of the latter equation below.

The topological term, describing the electromagnetic response of Weyl semimetals (and 3D TIs as well), may be regarded as being a consequence of the chiral anomaly [29,33–37], a fundamentally important concept in relativistic field theory, which has recently found its way into condensed matter physics and plays an important role in the modern understanding of topologically nontrivial phases of matter [38,39]. However, when using field theory concepts in the condensed matter context, one needs to exercise some care. Relativistic field theories possess exact symmetries, which in condensed matter systems may only be approximate. In particular, the chiral anomaly is closely related to chiral symmetry, i.e., separate conservation of fermions of left and right chirality, which is an exact symmetry in theories of massless relativistic particles. The chiral anomaly refers to violation of this symmetry by quantum effects in the presence of the electromagnetic field. In real Weyl or Dirac semimetals this symmetry may exist only approximately, if the Fermi energy is sufficiently close to the location of the nodes, so that the band dispersion may be taken to be linear to a good approximation. It is then unclear to what extent the concept of the chiral anomaly is meaningful, when applied to Weyl and Dirac semimetals.

In fact, the first sign of trouble with Eq. (7) is its immediate consequence, Eq. (9), which describes the CME. This equation has the appearance of a current, driven by an applied magnetic field in the presence of an energy separation between the nodes. Such an energy separation may exist in equilibrium in a noncentrosymmetric material [40], which leads one to a problematic conclusion that Eq. (9) describes an equilibrium current. This would violate basic principles of condensed matter physics and cannot happen [41]. The origin of this problem is precisely the relativistic invariance, assumed in the derivation of Eq. (7) [29], but not actually present in a real Weyl or Dirac semimetal. As was shown in Ref. [42], in a condensed matter setting, the response, described by Eq. (9), depends on the order in which the limits of zero frequency and zero wave vector are taken. When the frequency is taken to zero before the wave vector is taken to zero, which corresponds to the thermodynamic equilibrium response, the current vanishes. However, when the order of limits is reversed, which corresponds to the dc limit of nonequilibrium response, the current is nonzero and given by Eq. (9). This dependence on the order of limits appears to violate Lorentz invariance and thus should not happen in a relativistic particle physics context (at least if Lorentz invariance is assumed to be a fundamental symmetry). This highlights the importance of being careful when using low-energy models, exhibiting "relativistic" properties, to describe Weyl semimetals and other Dirac materials.

In this paper we will describe observable effects of the chiral anomaly, in particular the observable manifestation of the CME, in model Dirac and Weyl metals, i.e., lightly doped Dirac and Weyl semimetals. In accordance with the discussion above, we will use models for both which explicitly do not possess chiral symmetry and are thus free of the artifacts of "relativistic" low-energy models. We will demonstrate that in both Dirac and Weyl metals the main experimentally observable consequence of the CME is an unusual weak-field longitudinal magnetoresistance, which is negative, quadratic in the magnetic field, and large when the Fermi energy is sufficiently close to the Dirac or Weyl nodes [43]. A shorter account of this work, devoted specifically to the Weyl metal case, has already been published [44,45]. The rest of the paper is organized as follows. In Sec. II we introduce the model we will use to describe both Dirac and Weyl metals, and which is based on the TI-NI heterostructure model of Weyl semimetals, introduced by us before [3]. This model is the simplest model of a Dirac or Weyl metal that does not suffer from the "relativistic" artifacts; in particular it does not possess the spurious chiral symmetry of low-energy models with purely linear dispersion. In Sec. III we describe how the CME manifests in Dirac metals. We derive coupled transport equations for, using field theory terminology, the vector and the axial (chiral) charge densities, which are coupled in the presence of an applied magnetic field. The coupling is shown to be the manifestation of the CME. However, we demonstrate that this only leads to experimentally measurable consequences when a second ingredient is present: near conservation of the axial charge density, which is never exact, but becomes more and more precise as the Fermi energy

approaches the Dirac node. In Sec. IV we describe the same effect in Weyl semimetals. The manifestation of CME in Weyl semimetals is found to be nearly identical to the Dirac semimetals; i.e., whether the nodes are separated in momentum space or not does not matter for this effect. This appears to not be fully appreciated in the literature. We conclude in Sec. V with a brief discussion of our main results and experimental observability of the effect.

II. MODEL AND PRELIMINARIES

We start from a model of Weyl and Dirac metals, based on a TI-NI multilayer heterostructure, introduced by us [3]. The advantage of this model is that it is extremely simple, yet more realistic than the most generic low-energy model of a Dirac or Weyl metal would be; in particular it does not have the unphysical chiral symmetry. Since the model has already been described in a number of publications, here we will only recap the most essential points. The momentum-space Hamiltonian, describing the multilayer structure, is given by

$$H = v_F \tau^z (\hat{z} \times \boldsymbol{\sigma}) \cdot \mathbf{k} + \hat{\Delta}(k_z). \tag{10}$$

Here $\hat{z}$ is the growth direction of the heterostructure, v_F is the Fermi velocity, associated with the motion in the transverse (x,y) directions, $\boldsymbol{\sigma}$ are Pauli matrices, describing the real-spin degree of freedom, while $\boldsymbol{\tau}$ is the pseudospin, describing the top and bottom surfaces of TI layers in the heterostructure. The operator $\hat{\Delta}(k_z)$ describes the electron dynamics in the growth direction and is explicitly given by

$$\hat{\Delta}(k_z) = \Delta_S \tau^x + \frac{\Delta_D}{2}(\tau^+ e^{ik_z d} + \text{H.c.}), \tag{11}$$

where $\Delta_{S,D}$ are amplitudes for tunneling between top and bottom surfaces of the same (S) or neighboring (D) TI layers and d is the superlattice period. We will take them both to be positive for concreteness. This structure is an ordinary insulator when $\Delta_S > \Delta_D$ and a strong 3D TI otherwise. The point $\Delta_S = \Delta_D$ marks the TI-NI phase transition. At this point the structure is a Dirac semimetal. A Weyl semimetal is obtained by adding a TR breaking term $b\sigma^z$, which arises physically either from polarized magnetic impurities or an external magnetic field. This has been described in our earlier papers [3,46], and we will not dwell on it further.

To make contact with the chiral anomaly, it is useful to recast Eq. (10) in a "relativistic" form. To this end we expand Eq. (10) to leading order in the crystal momentum near the point $\mathbf{k} = (0,0,\pi/d)$, at which the gap closing occurs at the TI-NI transition when $\Delta_S = \Delta_D$. We obtain

$$H = v_F \tau^z (\hat{z} \times \boldsymbol{\sigma}) \cdot \mathbf{k} + \Delta_D d \tau^y k_z + (\Delta_S - \Delta_D)\tau^x. \tag{12}$$

This implies the following representation of the first four Dirac gamma matrices:

$$\gamma^0 = \tau^x,\ \gamma^1 = i\tau^y\sigma^y,\ \gamma^2 = -i\tau^y\sigma^x,\ \gamma^3 = i\tau^z. \tag{13}$$

The fifth gamma matrix,

$$\gamma^5 = i\gamma^0\gamma^1\gamma^2\gamma^3 = \tau^y\sigma^z, \tag{14}$$

defines the axial charge operator $n_a = \gamma^5 = \tau^y\sigma^z$. Absorbing the Fermi velocities v_F and $\tilde{v}_F = \Delta_D d$ into the definition of the corresponding momentum components and replacing $k^\mu \to -i\partial_\mu$, one obtains the following "relativistic" Lagrangian:

$$\mathcal{L} = \psi^\dagger i\partial_t \psi - H = \bar{\psi}\,[i\gamma^\mu(\partial_\mu + ieA_\mu + ib_\mu\gamma^5) - m]\psi. \tag{15}$$

Here $m = \Delta_S - \Delta_D$ is the Dirac "mass", $\bar{\psi} = \psi^\dagger\gamma^0$ is the Dirac adjoint of the Grassmann field ψ, A_μ is the electromagnetic gauge potential, and we have also introduced the chiral gauge field b_μ. Explicitly, the chiral gauge field arises from the following terms, added to the Hamiltonian Eq. (12):

$$H_b = b_0\tau^y\sigma^z + b_1\tau^x\sigma^x + b_2\tau^x\sigma^y + b_3\sigma^z. \tag{16}$$

The first term in Eq. (16) is clearly an axial chemical potential term, which shifts the left- (L) and right-handed (R) components of the Dirac fermion in opposite directions in energy. The last term is magnetization (or magnetic field) in the z direction, which shifts the L and R components in opposite directions in momentum space along the z axis. The second and third terms have the same symmetry as magnetization components in the x,y directions, and thus may be regarded as such. However, one needs to be aware that bare $\sigma^{x,y}$ operators will have a very different effect on the spectrum, creating a nodal line state rather than point nodes [46].

The chiral anomaly refers to anomalous nonconservation of the axial current $J_5^\mu = \bar{\psi}\gamma^\mu\gamma^5\psi$. This means that the axial current continuity equation has the following form:

$$\partial_\mu J_5^\mu = 2im\,\bar{\psi}\gamma^5\psi + \frac{e^2}{16\pi^2}\epsilon^{\mu\nu\alpha\beta}F_{\mu\nu}F_{\alpha\beta}. \tag{17}$$

The first term on the right-hand side of Eq. (17) is the classical contribution to the axial charge continuity equation, which is easily obtained from the Dirac equation. When the mass $m = 0$, i.e., when $\Delta_S = \Delta_D$, this term vanishes. This is an expression of chiral symmetry; i.e., classically the axial charge is conserved when $m = 0$. This conservation is violated when the continuity equation is evaluated in the second-quantized theory, which is where the second term comes from. However, $m = 0$ when $\Delta_S = \Delta_D$ is only obtained at leading order in the expansion of the operator $\hat{\Delta}(k_z)$ near $k_z = \pi/d$. In fact, m is a function of k_z and does not generally vanish. This means that the chiral symmetry is always only approximate and the axial charge is never a truly conserved quantity, even when the anomaly term is neglected. It is then clear that anomaly-related effects may only be observable if chiral symmetry is almost there, i.e., the axial charge relaxation time is long. We generally expect it to be long when the Fermi energy is close to zero, and thus the effect of higher order terms in the expansion of $\hat{\Delta}(k_z)$ is not significant. The purpose of the rest of the paper is to make these statements quantitative and evaluate the axial relaxation time explicitly for model Dirac and Weyl metals, described by Eq. (10).

III. ANOMALOUS DENSITY RESPONSE IN A DIRAC METAL

In this section, starting from a microscopic model of a Dirac semimetal, given by Eq. (10), we will derive transport equations for the vector and axial charge densities, in the presence of an external magnetic field. As will be demonstrated, the

chiral anomaly will manifest in these equations as a coupling between the vector and the axial charge densities, induced by the magnetic field. We will discuss under what conditions this coupling leads to observable transport phenomena, namely quadratic negative magnetoresistance.

We start from the Hamiltonian Eq. (10), with an added magnetic field in the z direction:

$$H = v_F \tau^z (\hat{z} \times \boldsymbol{\sigma}) \cdot (-i\boldsymbol{\nabla} + e\mathbf{A}) + \hat{\Delta}(k_z). \tag{18}$$

We will adopt the Landau gauge for the vector potential $\mathbf{A} = xB\hat{y}$ and ignore the Zeeman splitting in this section. The restriction of the magnetic field to the z direction simplifies calculations in the context of our model, but is otherwise nonessential. After a canonical transformation

$$\sigma^{\pm} \to \tau^z \sigma^{\pm}, \ \tau^{\pm} \to \sigma^z \tau^{\pm}, \tag{19}$$

Eq. (18) is easily diagonalized. The eigenvalues have the form

$$\epsilon_{na}(k_z) = s\sqrt{2\omega_B^2 n + \Delta^2(k_z)} \equiv s\epsilon_n(k_z). \tag{20}$$

Here $n \geqslant 1$ is the main Landau level (LL) index, k_y is the intra-LL orbital label, $s = \pm$ labels the two sets of positive and negative energy (or electron-like and hole-like) eigenvalues, $\omega_B = v_F/\ell_B$ is the Dirac cyclotron frequency, and $\ell_B = 1/\sqrt{eB}$ is the magnetic length. The index a is a composite index $a = s,t$, where $t = \pm$ labels two components of the Kramers doublet. The energy eigenvalues do not depend on t as we have ignored the Zeeman splitting due to the applied field. $t\Delta(k_z)$ are the two eigenvalues of the $\hat{\Delta}(k_z)$ operator, where $\Delta(k_z) = \sqrt{\Delta_S^2 + \Delta_D^2 + 2\Delta_S\Delta_D \cos(k_z d)}$. The corresponding eigenstates have the following form:

$$|n,a,k_y,k_z\rangle = \sum_{\tau} \left[z^a_{n\uparrow\tau}(k_z)|n-1,k_y,k_z,\uparrow,\tau\rangle + z^a_{n\downarrow\tau}(k_z)|n,k_y,k_z,\downarrow,\tau\rangle \right], \tag{21}$$

where

$$\langle \mathbf{r}|n,k_y,k_z,\sigma,\tau\rangle = \frac{1}{\sqrt{L_z}} e^{ik_z z} \phi_{nk_y}(\mathbf{r})|\sigma,\tau\rangle, \tag{22}$$

$\phi_{nk_y}(\mathbf{r})$ are the Landau-gauge orbital wave functions, and σ,τ are the spin and the top-bottom surface pseudospin labels, respectively. The four-component eigenvector $|z^a_n(k_z)\rangle$ may be written as a tensor product of the two-component spin and pseudospin eigenvectors, i.e., $|z^a_n(k_z)\rangle = |v^a_n(k_z)\rangle \otimes |u^a(k_z)\rangle$, where

$$\begin{aligned} |v^{\rm st}_n(k_z)\rangle &= \frac{1}{\sqrt{2}} \left(\sqrt{1 + s\frac{t\Delta(k_z)}{\epsilon_n(k_z)}}, -is\sqrt{1 - s\frac{t\Delta(k_z)}{\epsilon_n(k_z)}} \right), \\ |u^t(k_z)\rangle &= \frac{1}{\sqrt{2}} \left(1, t\frac{\Delta_S + \Delta_D e^{-ik_z d}}{\Delta(k_z)} \right). \end{aligned} \tag{23}$$

The lowest $n = 0$ LL is special, which is a consequence of nontrivial Berry curvature. The s quantum number is absent in this case and taking $B > 0$ for concreteness, we have

$$\epsilon_{nt}(k_z) = -t\Delta(k_z), \tag{24}$$

and $|v^t_0(k_z)\rangle = (0,1)$.

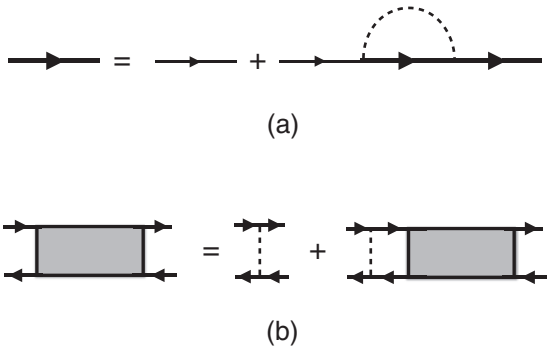

FIG. 1. (a) Graphical representation of the SCBA equation. Regular lines denote bare Green's functions, while bold lines correspond to impurity-averaged Green's functions. Dashed line denotes impurity averaging. (b) Graphical representation of the diffusion propagator, which is the sum of all ladder diagrams. Bold lines correspond to impurity-averaged Green's functions.

We model the potential due to random impurities as Gaussian white noise potential with $\langle V(\mathbf{r})\rangle = 0$ and

$$\langle V(\mathbf{r})V(\mathbf{r}')\rangle = \gamma^2 \delta(\mathbf{r} - \mathbf{r}'). \tag{25}$$

For simplicity we assume that the impurity potential is independent of the pseudospin index τ, which physically means that we ignore scattering between the top and botton surfaces of the TI layers. This does not affect the results qualitatively and is only done to simplify calculations.

The impurity scattering may be treated by the standard diagrammatic perturbation theory. In the self-consistent Born approximation (SCBA) one obtains the following expression for the retarded impurity self-energy [see Fig. 1(a) for graphical representation]:

$$\Sigma^R_{na}(k_z,\omega) = \frac{1}{L_z} \sum_{n'a'k'_y k'_z} \langle |\langle nak_y k_z|V|n'a'k'_y k'_z\rangle|^2 \rangle \times G^R_{n'a'}(k'_z,\omega), \tag{26}$$

where

$$G^R_{na}(k_z,\omega) = \frac{1}{\omega - \xi_{na}(k_z) + i\eta} \tag{27}$$

is the retarded Green's function of a clean Dirac metal (full self-consistency is unnecessary here) and $\xi_{na}(k_z) = \epsilon_{na}(k_z) - \epsilon_F$. We will assume that the Fermi energy $\epsilon_F > 0$, i.e., that the Dirac semimetal is electron-doped. Matrix elements of the impurity potential between the LL eigenstates are easily evaluated and are given by

$$\begin{aligned} &\langle nak_y k_z|V|n'a'k'_y k'_z\rangle \\ &= \frac{1}{L_x L_y L_z} \sum_{\mathbf{q}} V(\mathbf{q}) \delta_{q_y,k_y-k'_y} \delta_{q_z,k_z-k'_z} e^{iq_x \ell_B^2 (k_y+k'_y)/2} \\ &\times \sum_{\tau} \left[\bar{z}^a_{n\uparrow\tau}(k_z) z^{a'}_{n'\uparrow\tau}(k'_z) F_{n-1,n'-1}(\mathbf{q}) \right. \\ &\left. + \bar{z}^a_{n\downarrow\tau}(k_z) z^{a'}_{n'\downarrow\tau}(k'_z) F_{n,n'}(\mathbf{q}) \right], \end{aligned} \tag{28}$$

where the LL form factors have the following well-known form,

$$F_{n,n'}(\mathbf{q}) = \sqrt{\frac{n'!}{n!}}\left(\frac{iq_x\ell_B - q_y\ell_B}{2}\right)^{n-n'} e^{-q^2\ell_B^2/4} L_{n'}^{n-n'}\left(\frac{q^2\ell_B^2}{2}\right), \tag{29}$$

and $L_{n'}^{n-n'}(x)$ are the generalized Laguerre polynomials. Using the following properties of the LL form factor momentum integrals,

$$\int \frac{d^2q}{(2\pi)^2} F_{n,n'}(\mathbf{q})F_{n',n}(-\mathbf{q}) = \frac{1}{2\pi\ell_B^2},$$
$$\int \frac{d^2q}{(2\pi)^2} F_{n,n'}(\mathbf{q})F_{n'-1,n-1}(-\mathbf{q}) = 0, \tag{30}$$

we obtain

$$\begin{aligned}&\Gamma_{na,n'a'}(k_z,k_z')\\ &\quad\equiv \langle|\langle nak_yk_z|V|n'a'k_y'k_z'\rangle|^2\rangle\\ &\quad= \gamma^2\left[\left|v_{n\uparrow}^a(k_z)\right|^2\left|v_{n'\uparrow}^{a'}(k_z')\right|^2 + \left|v_{n\downarrow}^a(k_z)\right|^2\left|v_{n'\downarrow}^{a'}(k_z')\right|^2\right]\\ &\qquad\times|\langle u^a(k_z)|u^{a'}(k_z')\rangle|^2.\end{aligned} \tag{31}$$

The SCBA equation then takes the form

$$\Sigma_{na}^R(k_z,\omega) = \frac{1}{2\pi\ell_B^2 L_z}\sum_{n'a'k_z'}\Gamma_{na,n'a'}(k_z,k_z')G_{n'a'}^R(k_z',\omega). \tag{32}$$

At this point we will assume that ϵ_F is sufficiently large, so that scattering between the electron- and hole-like LLs may be neglected. Then the negative energy $s=-$ states do not contribute and we will ignore them henceforth. We will also drop the explicit $s=+$ index, since all states are the $s=+$ states, and replace the a index with t from now on.

The SCBA equation may now be solved analytically. Using

$$\mathrm{Im}G_{nt}^R(k_z,\omega) = -\pi\delta[\epsilon_n(k_z)-\epsilon_F], \tag{33}$$

it is easy to see that the dependence of the matrix element $\Gamma_{nt,n't'}(k_z,k_z')$ on the LL indices n,n' in fact drops out, since this dependence only enters through the LL energies $\epsilon_n(k_z)$, which may simply be replaced by the Fermi energy. We then obtain the following expression for the impurity scattering rate:

$$\begin{aligned}\frac{1}{\tau(k_z)} &\equiv -2\mathrm{Im}\Sigma_{nt}^R(k_z,\omega)\\ &= \frac{1}{\tau_0}\left[1+\frac{\Delta_S+\Delta_D\cos(k_zd)}{\epsilon_F}\frac{\Delta_S+\Delta_D\langle\cos(k_zd)\rangle}{\epsilon_F}\right].\end{aligned} \tag{34}$$

Here

$$\frac{1}{\tau_0} = \frac{1}{2}\pi\gamma^2 g(\epsilon_F), \tag{35}$$

and $g(\epsilon_F)$ is the total density of states at Fermi energy. Explicitly,

$$\begin{aligned}g(\epsilon_F) &= \frac{1}{2\pi\ell_B^2}\int_{-\pi/d}^{\pi/d}\frac{dk_z}{2\pi}\sum_{nt}\delta[\epsilon_n(k_z)-\epsilon_F)]\\ &= \frac{\epsilon_F}{\pi v_F^2}\int_{-\pi/d}^{\pi/d}\frac{dk_z}{2\pi}\Theta[\epsilon_F-\Delta(k_z)],\end{aligned} \tag{36}$$

where in the second line above we have assumed that the magnetic field is weak and converted the sum over the LL index n to an integral. Finally, $\langle\cos(k_zd)\rangle$ in Eq. (34) means the average of $\cos(k_zd)$ over the Fermi surface, which is defined as

$$\langle\cos(k_zd)\rangle = \frac{2}{g(\epsilon_F)}\int_{-\pi/d}^{\pi/d}\frac{dk_z}{2\pi}\sum_n\cos(k_zd)\delta[\epsilon_n(k_z)-\epsilon_F)]. \tag{37}$$

We will use this definition of Fermi surface averages throughout the paper. Evaluating the average in Eq. (37) in the weak-field limit, one obtains

$$\langle\cos(k_zd)\rangle = -\frac{1}{k_0d}\sqrt{1-\left(\frac{\Delta_S^2+\Delta_D^2-\epsilon_F^2}{2\Delta_S\Delta_D}\right)^2}, \tag{38}$$

where

$$k_0 = \frac{1}{d}\arccos\left(\frac{\Delta_S^2+\Delta_D^2-\epsilon_F^2}{2\Delta_S\Delta_D}\right) \tag{39}$$

is the solution of the equation $\Delta(k_z)=\epsilon_F$ modulo π/d.

At this point we will specialize to the case of a Dirac metal, i.e., set $\Delta_S=\Delta_D$, which makes the Dirac mass at the point $k_x=k_y=0,k_z=\pi/d$ vanish. We will also assume that the Fermi energy is close to the Dirac point, which means $\epsilon_F/\Delta_S \ll 1$ (but still far enough that $\epsilon_F\tau_0 \gg 1$). Then we obtain

$$\langle\cos(k_zd)\rangle \approx -1+\frac{\epsilon_F^2}{6\Delta_S^2}+\frac{\epsilon_F^4}{180\Delta_S^4}+\cdots, \tag{40}$$

and it is clear that, to leading order in the small parameter ϵ_F/Δ_S,

$$\frac{1}{\tau(k_z)} \approx \frac{1}{\tau_0}. \tag{41}$$

We now want to find the propagator of the diffusion modes in our system, which correspond to nearly conserved physical quantities with long (i.e., much longer than τ_0) relaxation times. In the limit $\epsilon_F\tau_0 \gg 1$, the diffusion propagator may be evaluated by summing ladder impurity scattering diagrams, as shown in Fig. 1(b) [47]. This approximation (self-consistent noncrossing approximation) is consistent with the SCBA for the impurity self-energy, in the sense that together they preserve exact conservation laws, in particular charge conservation. The diffusion propagator (or diffuson), evaluated in the self-consistent noncrossing approximation, takes the following form:

$$\mathcal{D}(\mathbf{q},\Omega) = [1-I(\mathbf{q},\Omega)]^{-1}, \tag{42}$$

where $I(\mathbf{q},\Omega)$ is a 16×16 matrix with respect to the combined spin and pseudospin indices $\alpha=\sigma,\tau$, which has the following explicit form:

$$\begin{aligned}I_{\alpha_1\alpha_2,\alpha_3\alpha_4}(\mathbf{q},\Omega) = \frac{\gamma^2}{L_xL_yL_z}\int d^3rd^3r'e^{-i\mathbf{q}\cdot(\mathbf{r}-\mathbf{r}')}\\ \times G_{\alpha_1\alpha_3}^R(\mathbf{r},\mathbf{r}'|\Omega)G_{\alpha_4\alpha_2}^A(\mathbf{r}',\mathbf{r}|0).\end{aligned} \tag{43}$$

The Green's functions appearing in Eq. (43) are the impurity-averaged SCBA retarded and advanced Green's functions,

found above:

$$G^{R,A}_{\alpha\alpha'}(\mathbf{r},\mathbf{r}'|\Omega)=\sum_{ntk_yk_z}\frac{\langle\mathbf{r}\alpha|ntk_yk_z\rangle\langle ntk_yk_z|\mathbf{r}'\alpha'\rangle}{\Omega-\xi_{nt}(k_z)\pm i/2\tau_0}, \quad (44)$$

where

$$\langle\mathbf{r}\alpha|ntk_yk_z\rangle=\frac{1}{\sqrt{L_z}}e^{ik_zz}z^t_{n\alpha}(k_z)\phi_{nk_y}(\mathbf{r}). \quad (45)$$

Evaluating $I(\mathbf{q},\Omega)$ in the general case is a formidable task, mostly due to the presence of the LL index sums. LLs with different n will generally be mixed by impurity scattering, in which case analytical evaluation of Eq. (43) becomes impossible. However, we are primarily interested in transport along the direction of the applied magnetic field, i.e., the z direction. If, in accordance with this, we set $\mathbf{q}=q\hat{z}$, it is easy to see that only a single LL index sum remains in Eq. (43) after integration over the x,y coordinates. In this case we obtain

$$I_{\alpha_1\alpha_2,\alpha_3\alpha_4}(q,\Omega)=\frac{\gamma^2}{2\pi\ell_B^2L_z}\sum_{ntt'k_z}\frac{z^t_{n\alpha_1}(k_z)\bar{z}^t_{n\alpha_3}(k_z)}{\Omega-\xi_{nt}(k_z+q/2)+i/2\tau_0}\times\frac{z^{t'}_{n\alpha_4}(k_z)\bar{z}^{t'}_{n\alpha_2}(k_z)}{-\xi_{nt'}(k_z-q/2)-i/2\tau_0}. \quad (46)$$

The dependence of the eigenfunctions $z^t_{n\alpha}(k_z)$ on q has been neglected in Eq. (46), since the corresponding terms are subdominant in the limit $\epsilon_F\tau_0\gg1$ and $qv_F\tau_0\ll1$.

At this point we need to explicitly separate out the part of the diffusion propagator that corresponds to hydrodynamic modes, i.e., modes with long relaxation times. On physical grounds, we expect only two such modes to be present in our system, corresponding to the diffusion of the vector $n_v=\sigma^0\tau^0$ and the axial $n_a=\sigma^z\tau^y$ charges. Note that the axial charge operator changes to $n_a=\sigma^0\tau^y$ after the canonical transformation Eq. (19). The projection onto the vector-axial charge subspace is accomplished by the following transformation:

$$\mathcal{D}^{-1}_{ab}=\tfrac{1}{4}(\sigma\tau)^a_{\alpha_2\alpha_1}\mathcal{D}^{-1}_{\alpha_1\alpha_2,\alpha_3\alpha_4}(\sigma\tau)^b_{\alpha_3\alpha_4}, \quad (47)$$

where a,b refer to either the vector or the axial charge and summation over repeated indices is implied. The projected inverse diffusion propagator is a 2×2 matrix. Its diagonal components describe the independent transport of the vector and axial charge densities, while the off-diagonal components describe their coupling, induced by the applied magnetic field. Let us first evaluate the off-diagonal component (the two off-diagonal components are equal by reciprocity). We have

$$\mathcal{D}^{-1}_{va}(\mathbf{q},\Omega)=-\frac{1}{4}(\sigma^0\tau^0)_{\alpha_2\alpha_1}I_{\alpha_1\alpha_2,\alpha_3\alpha_4}(\mathbf{q},\Omega)(\sigma^0\tau^y)_{\alpha_3\alpha_4}=-\frac{\gamma^2}{8\pi\ell_B^2L_z}\sum_{ntt'k_z}\frac{\langle z^{t'}_n(k_z)|z^t_n(k_z)\rangle}{\Omega-\xi_{nt}(k_z+q/2)+i/2\tau_0}\times\frac{\langle z^t_n(k_z)|\tau^y|z^{t'}_n(k_z)\rangle}{-\xi_{nt'}(k_z-q/2)-i/2\tau_0}. \quad (48)$$

Since $\langle z^t_n(k_z)|z^{t'}_n(k_z)\rangle=\delta_{tt'}$, and

$$\langle z^t(k_z)|\tau^y|z^t(k_z)\rangle=-t\frac{\Delta_D\sin(k_zd)}{\Delta(k_z)}, \quad (49)$$

it is clear that LLs with $n\geqslant1$ cannot contribute to Eq. (48), since their energies $\epsilon_{nt}(k_z)$ do not depend on the index t, which leads to an exact cancellation of contributions with $t=\pm$. The $n=0$ LL, on the other hand, does contribute, since the corresponding eigenstate energies do depend on t, as seen in Eq. (24). When $\epsilon_F>0$, it is clear that only the $t=-$ lowest LL contributes to Eq. (48), since only this LL crosses the Fermi energy. Using an identity

$$AB=\frac{B-A}{A^{-1}-B^{-1}}, \quad (50)$$

we have

$$\frac{1}{\Omega-\xi_{0-}(k_z+q/2)+i/2\tau_0}\frac{1}{-\xi_{0-}(k_z-q/2)-i/2\tau_0}=\frac{1}{\Omega-\xi_{0-}(k_z+q/2)+\xi_{0-}(k_z-q/2)+i/\tau_0}\times\left[\frac{1}{-\xi_{0-}(k_z-q/2)-i/2\tau_0}-\frac{1}{\Omega-\xi_{0-}(k_z+q/2)+i/2\tau_0}\right]\approx\frac{2\pi i\,\delta[\Delta(k_z)-\epsilon_F]}{\Omega-q\frac{d\Delta}{dk_z}+i/\tau_0}. \quad (51)$$

Substituting this into Eq. (48) and expanding to first order in Ω and q, we obtain

$$\mathcal{D}^{-1}_{va}(\mathbf{q},\Omega)=\frac{\gamma^2\tau_0}{8\pi\ell_B^2}\int_{-\pi/d}^{\pi/d}dk_z\frac{1}{\Delta_Sd}\frac{d\Delta}{dk_z}\delta[\Delta(k_z)-\epsilon_F]\times\left(1+i\Omega\tau_0-iq\frac{d\Delta}{dk_z}\tau_0\right), \quad (52)$$

where we have used

$$\frac{d\Delta}{dk_z}=-\frac{\Delta_S\Delta_Dd\sin(k_zd)}{\Delta(k_z)}=-\Delta_Sd\langle z^-(k_z)|\tau^y|z^-(k_z)\rangle. \quad (53)$$

Since $d\Delta/dk_z$ is an odd function of k_z with respect to the point $k_z=\pi/d$, it is clear that only the term, proportional to q, survives the integration over k_z in Eq. (52). Then we obtain

$$\mathcal{D}^{-1}_{va}(\mathbf{q},\Omega)=-iq\frac{\gamma^2\tau_0^2}{4\pi\ell_B^2\Delta_Sd}\left|\frac{d\Delta}{dk_z}\right|_{k_z=k_z^\pm}, \quad (54)$$

where $k_z^\pm=\pi/d\pm k_0$ are the two solutions of the equation $\Delta(k_z)=\epsilon_F$. Evaluating the lowest LL Fermi velocity $d\Delta/dk_z$ explicitly, we obtain

$$\left|\frac{d\Delta}{dk_z}\right|_{k_z=k_z^\pm}=\frac{d}{2}\sqrt{4\Delta_S^2-\epsilon_F^2}\approx\Delta_Sd. \quad (55)$$

Then, using $\gamma^2=2/\pi g(\epsilon_F)\tau_0$, we finally obtain

$$\mathcal{D}^{-1}_{va}(\mathbf{q},\Omega)=\mathcal{D}^{-1}_{av}(\mathbf{q},\Omega)=-iq\tau_0\frac{eB}{2\pi^2g(\epsilon_F)}\equiv-iq\tau_0\Gamma. \quad (56)$$

The coefficient Γ in Eq. (56) is a new transport coefficient that describes the lowest LL-mediated coupling between the vector

and the axial charge densities. This coupling may be regarded as being a consequence of the chiral anomaly.

The diagonal elements of the inverse diffusion propagator correspond to independent transport and relaxation of the vector and axial charge densities. These are nonzero in the absence of the magnetic field and we will thus evaluate them in the limit $B \to 0$, since we are interested in weak-field transport here. Accordingly, the contribution of the lowest LL is negligible in this case and we will ignore it. The limit of $B \to 0$ will be taken after summing the contributions of all the $n \geqslant 1$ LLs. One obtains

$$\mathcal{D}_{vv}^{-1}(\mathbf{q},\Omega) = 1 - \frac{\gamma^2\tau_0}{4\pi\ell_B^2}\sum_{n\geqslant 1}\int_{-\pi/d}^{\pi/d} dk_z \frac{\delta[\epsilon_n(k_z)-\epsilon_F]}{1 - i\Omega\tau_0 + iq\tau_0\frac{\Delta}{\epsilon_F}\frac{d\Delta}{dk_z}}. \tag{57}$$

The sum over the LL index n may be done in the limit $B \to 0$ by converting the sum into an integral, just as was done when solving the SCBA equation above. Performing the integral and expanding to leading nonvanishing order in Ω and q, one obtains

$$\mathcal{D}_{vv}^{-1}(\mathbf{q},\Omega) = -i\Omega\tau_0 + q^2\tau_0^2\left\langle\left(\frac{\Delta}{\epsilon_F}\frac{d\Delta}{dk_z}\right)^2\right\rangle, \tag{58}$$

where the angular brackets denote average over the Fermi surface, defined as in Eq. (37). Using

$$\Delta\frac{d\Delta}{dk_z} = \frac{1}{2}\frac{d\Delta^2}{dk_z} = -\Delta_S\Delta_D\sin(k_z d), \tag{59}$$

the average is easily evaluated and we obtain

$$\left\langle\left(\frac{\Delta}{\epsilon_F}\frac{d\Delta}{dk_z}\right)^2\right\rangle \approx \frac{1}{3}(\Delta_S d)^2. \tag{60}$$

Defining the z-direction diffusion coefficient as $D = (\Delta_S d)^2\tau_0/3$, we finally obtain

$$\mathcal{D}_{vv}^{-1}(\mathbf{q},\Omega) = -i\Omega\tau_0 + Dq^2\tau_0. \tag{61}$$

This has the expected form for the inverse diffusion propagator of a conserved quantity. Namely, the full diffusion propagator $\mathcal{D}(\mathbf{q},\Omega)$ will exhibit a diffusion pole at $\Omega,q \to 0$ as a consequence of an exact conservation of the vector charge.

Finally, we need to evaluate $\mathcal{D}_{aa}^{-1}$. Here we expect that the diffusion pole will be absent due to a finite relaxation rate for the axial charge density, since it is not an exactly conserved quantity. We obtain

$$\mathcal{D}_{aa}^{-1}(\mathbf{q},\Omega) = 1 - \frac{\gamma^2\tau^0}{8\pi\ell_B^2}\sum_{n\geqslant 1,tt'}\int_{-\pi/d}^{\pi/d} dk_z \left|\left\langle z_n^t(k_z)\right|\tau_y\left|z_n^{t'}(k_z)\right\rangle\right|^2 \times \frac{\delta[\epsilon_n(k_z)-\epsilon_F]}{1 - i\Omega\tau_0 + iq\tau_0\frac{\Delta}{\epsilon_F}\frac{d\Delta}{dk_z}}. \tag{62}$$

Evaluating the matrix element in Eq. (62), one obtains

$$\frac{1}{2}\sum_{tt'}\left|\left\langle z_n^t(k_z)\right|\tau_y\left|z_n^{t'}(k_z)\right\rangle\right|^2 = 1 - \frac{\Delta^2(k_z) - \Delta_D^2\sin^2(k_z d)}{\epsilon_n^2(k_z)}. \tag{63}$$

Substituting this back into Eq. (62) and evaluating the sum over the LL index by converting it to an integral, as before, and expanding to leading nonvanishing order in Ω and q, we get

$$\mathcal{D}_{aa}^{-1}(\mathbf{q},\Omega) = 1 - \left\langle 1 - \frac{\Delta^2(k_z) - \Delta_D^2\sin^2(k_z d)}{\epsilon_F^2}\right\rangle(1 + i\Omega\tau_0) + q^2\tau_0^2\left\langle\left(1 - \frac{\Delta^2(k_z) - \Delta_D^2\sin^2(k_z d)}{\epsilon_F^2}\right)\left(\frac{\Delta}{\epsilon_F}\frac{d\Delta}{dk_z}\right)^2\right\rangle, \tag{64}$$

where the angular brackets again mean average over the Fermi surface. Evaluating the Fermi surface averages, assuming as before that $\epsilon_F/\Delta_S \ll 1$, we finally obtain

$$\mathcal{D}_{aa}^{-1}(\mathbf{q},\Omega) = -i\Omega\tau_0 + \frac{\tau_0}{\tau_a} + Dq^2\tau_0, \tag{65}$$

where

$$\frac{1}{\tau_a} = \frac{\epsilon_F^2}{20\Delta_S^2\tau_0} \tag{66}$$

is the axial charge relaxation rate. Equation (66) is one of the main results of this section. As expected, the axial charge is not exactly conserved, as the chiral symmetry is always explicitly violated in a real Dirac semimetal by nonlinearity of the band dispersion, which is necessarily present. However, since the band dispersion becomes more and more linear as the energy is reduced towards the Dirac point, the axial relaxation rate tends to zero as the Fermi energy goes to zero faster than the momentum relaxation rate $1/\tau_0$, which of course also vanishes in the limit $\epsilon_F \to 0$ due to the vanishing density of states. (This is true provided we neglect the influence of the magnetic field on the density of states. In principle, even in the limit $\epsilon_F \to 0$ there is a finite density of states, proportional to B. We ignore this in the weak-field limit.) Thus, near the Dirac point $\tau_a \gg \tau_0$, which expresses the near conservation of the axial charge due to the emergent low-energy chiral symmetry. As will be seen below, this is a necessary condition for a large negative magnetoresistance.

Collecting all the matrix elements, we obtain the following result for the full inverse diffusion propagator, which describes coupled transport of the vector and axial charge densities

$$\mathcal{D}^{-1}(q,\Omega) = \begin{pmatrix} -i\Omega\tau_0 + Dq^2\tau_0 & -iq\Gamma\tau_0 \\ -iq\Gamma\tau_0 & -i\Omega\tau_0 + \tau_0/\tau_a + Dq^2\tau_0 \end{pmatrix}. \tag{67}$$

Viewing Eq. (67) as the inverse Green's function of the diffusion equation for the vector and axial charges and performing the inverse Fourier transform, we obtain the coupled diffusion equations

$$\begin{aligned} \frac{\partial n_v}{\partial t} &= D\frac{\partial^2 n_v}{\partial z^2} + \Gamma\frac{\partial n_a}{\partial z}, \\ \frac{\partial n_a}{\partial t} &= D\frac{\partial^2 n_a}{\partial z^2} - \frac{n_a}{\tau_a} + \Gamma\frac{\partial n_v}{\partial z}. \end{aligned} \tag{68}$$

Since the vector charge is exactly conserved, the first equation must have the form of the continuity equation

$$\frac{\partial n_v}{\partial t} = -\nabla \cdot \mathbf{j}_v, \tag{69}$$

where $\mathbf{j}_v$ is the vector current, i.e., current of the vector charge. This leads to the following explicit expression for the vector current:

$$j_v = -\frac{\sigma_0}{e}\frac{\partial \mu_v}{\partial z} - \frac{e^2 B}{2\pi^2}\delta\mu_a. \tag{70}$$

Here μ_v and μ_a are the vector and axial electrochemical potentials, $\sigma_0 = e^2 g(\epsilon_F)D$ is the zero-field Drude conductivity, and we have used $\delta n_{v,a} = g(\epsilon_F)\delta\mu_{v,a}$. The first term in Eq. (70) is an ordinary current in response to a gradient of the electrochemical potential. The second term is a consequence of chiral anomaly and is an extra contribution to the current, proportional to the applied magnetic field and (nonequilibrium part of) the axial electrochemical potential. This is known as the CME in the literature [32], and this extra contribution is what leads to the anomalous negative longitudinal magnetoresistance. However, the CME by itself is only one component of the experimentally observable effect, i.e., the negative magnetoresistance. The second crucial component, without which the effect is unobservable, is contained in the second of Eq. (68). Namely, as will be seen shortly, the CME leads to observable magnetoresistance only if the axial charge relaxation rate $1/\tau_a$ is small; i.e., the axial charge is a nearly conserved quantity. As discussed above, this near conservation of the axial charge is a characteristic feature of Dirac (and Weyl) semimetals, which becomes more and more precise as the Fermi energy is reduced towards the Dirac (or Weyl) point.

To obtain the CME-related magnetoresistance explicitly, we now assume that there is a uniform steady state vector current density in the z direction j_v, present in the system. The second of Eqs. (68) then gives

$$\delta\mu_a = \Gamma\tau_a\frac{\partial \mu_v}{\partial z}. \tag{71}$$

Substituting this into the equation for the vector current Eq. (70), we obtain the following expression for the total diagonal conductivity:

$$\sigma_{zz} = \sigma_0 + \frac{e^4 B^2 \tau_a}{4\pi^4 g(\epsilon_F)}. \tag{72}$$

Thus the CME is manifested as a positive longitudinal magnetoconductivity (or negative magnetoresistivity), proportional to B^2. Crucially, it is also proportional to τ_a, and a large τ_a is thus necessary for this effect to be significant. The magnetoresistance is further enhanced when $\epsilon_F \to 0$ by vanishing of the density of states as $g(\epsilon_F) \sim \epsilon_F^2$.

IV. ANOMALOUS DENSITY RESPONSE IN A WEYL METAL

In this section we will extend the theory of the anomaly-related negative magnetoresistance, presented above, to the case of Weyl metals, where the individual Weyl fermion components of the Dirac fermion are separated to distinct points in momentum space. A shorter account of this work has already been presented in Refs. [44,45]. As the calculations are quite similar to the case of Dirac metals, described in the previous section, here we will only focus on the differences from the Dirac metal case and skip some of the details.

In the context of our model Dirac semimetal, described by Eq. (18), the separation of the Dirac fermion into Weyl fermions is most easily accomplished by adding a term $b\sigma^z$ to the Hamiltonian. Physically this term may arise from magnetized impurities, doped into the Dirac semimetal, or even from the Zeeman coupling to the applied magnetic field.

The LL energy eigenvalues now have the form

$$\epsilon_{na}(k_z) = s\sqrt{2\omega_B^2 n + m_t^2(k_z)} \equiv s\epsilon_{nt}(k_z),\ n \geqslant 1, \tag{73}$$

while

$$\epsilon_{0t}(k_z) = -m_t(k_z). \tag{74}$$

Here

$$m_t(k_z) = b + t\Delta(k_z). \tag{75}$$

Taking b to be nonnegative, $m_-(k_z)$ vanishes at two points along the z axis in momentum space, given by the two solutions of the equation

$$\Delta(k_z) = b. \tag{76}$$

The solutions are $k_z^{\pm} = \pi/d \pm k_0$, where

$$k_0 = \frac{1}{d}\arccos\left(\frac{\Delta_S^2 + \Delta_D^2 - b^2}{2\Delta_S\Delta_D}\right). \tag{77}$$

These correspond to the locations of the two Weyl nodes of opposite chirality on the z axis in momentum space. The nodes exist as long as $b_{c1} < b < b_{c2}$, where $b_{c1} = |\Delta_S - \Delta_D|$ and $b_{c2} = \Delta_S + \Delta_D$. The eigenvectors are given by

$$\begin{aligned} \left|v_n^{\mathrm{st}}(k_z)\right\rangle &= \frac{1}{\sqrt{2}}\left(\sqrt{1 + s\frac{m_t(k_z)}{\epsilon_{nt}(k_z)}}, -is\sqrt{1 - s\frac{m_t(k_z)}{\epsilon_{nt}(k_z)}}\right), \\ |u^t(k_z)\rangle &= \frac{1}{\sqrt{2}}\left(1, t\frac{\Delta_S + \Delta_D e^{-ik_z d}}{\Delta(k_z)}\right), \end{aligned} \tag{78}$$

while the $n = 0$ LL is polarized downwards, as before.

The main difference from the Dirac metal case is that the Kramers degeneracy between the $t = \pm$ states is now broken by the spin splitting term $b\sigma^z$. When b is sufficiently large (i.e., $b > \epsilon_F$), we may ignore the $t = +$ states entirely. Solving the SCBA equations as before, we obtain

$$\frac{1}{\tau(k_z)} = \frac{1}{\tau_0}\left[1 + \frac{m_-(k_z)\langle m_-\rangle}{\epsilon_F^2}\right], \tag{79}$$

where $1/\tau_0 = \pi\gamma^2 g(\epsilon_F)$ and

$$g(\epsilon_F) = \frac{1}{2\pi\ell_B^2}\int_{-\pi/d}^{\pi/d}\frac{dk_z}{2\pi}\sum_n \delta[\epsilon_{n-}(k_z) - \epsilon_F] \tag{80}$$

is the total density of states at Fermi energy. At the Weyl nodes $m_-(k_z)$ vanishes and changes sign. This implies that, for sufficiently small Fermi energy, such that the band dispersion in the z direction may be assumed to be linear to a good approximation, the Fermi surface average $\langle m_-(k_z)\rangle$ will vanish. This property has a simple geometrical interpretation. The Weyl nodes may be thought of as monopole sources of

Berry curvature, whose z component is proportional to $m_-(k_z)$. This clearly averages to zero when integrated over the volume, enclosed by a sufficiently small Fermi surface sheet, containing the node [48]. Assuming this to be the case, we obtain

$$\frac{1}{\tau(k_z)} \approx \frac{1}{\tau_0}. \tag{81}$$

Note that since the densities of states in Eqs. (36) and (80) are essentially identical in the limit of small Fermi energy (the twofold Kramers degeneracy in the Dirac metal case is replaced by two identical Fermi surfaces, enclosing the Weyl nodes, in the Weyl metal case), the impurity scattering rate in the Weyl metal is twice as large. This is easy to understand physically and follows simply from the near orthogonality of the $|u^{\pm}(k_z)\rangle$ eigenstates at small momentum difference, i.e., $\langle u^t(k_z)|u^{t'}(k_z')\rangle \approx \delta_{tt'}$, when $|k_z - k_z'|d \ll 1$, which means that scattering between the two components of the Kramers doublet is suppressed in the Dirac metal. This suppression disappears in the Weyl metal case, since in this case the two Fermi surfaces arise from states in the same $t = -$ band.

The evaluation of the diffusion propagator goes along exactly the same lines as before. The only difference is that only the $t = -$ states contribute; i.e., we have

$$I_{\alpha_1\alpha_2,\alpha_3\alpha_4}(q,\Omega) = \frac{\gamma^2}{2\pi\ell_B^2 L_z}\sum_{nk_z}\frac{z^-_{n\alpha_1}(k_z)\bar{z}^-_{n\alpha_3}(k_z)}{\Omega - \xi_{n-}(k_z+q/2)+i/2\tau_0} \times \frac{z^-_{n\alpha_4}(k_z)\bar{z}^-_{n\alpha_2}(k_z)}{-\xi_{n-}(k_z-q/2)-i/2\tau_0}. \tag{82}$$

For the same reason, the projection of the full diffusion propagator onto the vector and axial charge subspace differs by a factor of $1/2$ from the Dirac semimetal case

$$\mathcal{D}^{-1}_{ab} = \tfrac{1}{2}(\sigma\tau)^a_{\alpha_2\alpha_1}\mathcal{D}^{-1}_{\alpha_1\alpha_2,\alpha_3\alpha_4}(\sigma\tau)^b_{\alpha_3\alpha_4}. \tag{83}$$

The vector to axial charge coupling term arises, as before, entirely from the contribution of the $n = 0$ LL. We obtain

$$\mathcal{D}^{-1}_{va}(\mathbf{q},\Omega) = -iq\tau_0\frac{1}{2\pi\ell_B^2 g(\epsilon_F)\Delta_S d}\left|\frac{d\Delta}{dk_z}\right|_{k_z=k_z^{\pm}}, \tag{84}$$

where $k_z^{\pm}$ are now solutions of the equation

$$\Delta(k_z) = b + \epsilon_F, \tag{85}$$

which determines the points at which the Fermi energy intersects the $n = 0$, $t = -$ LL. One obtains

$$\left|\frac{d\Delta}{dk_z}\right|_{k_z=k_z^{\pm}} = \frac{d}{2(b+\epsilon_F)}\sqrt{\left[(b+\epsilon_F)^2 - b_{c1}^2\right]\left[b_{c2}^2 - (b+\epsilon_F)^2\right]}. \tag{86}$$

Assuming $b_{c1} \ll b + \epsilon_F \ll b_{c2}$, which implies that the Weyl node splitting and the Fermi energy are such that the band dispersion at the Fermi level may be taken to be linear, one obtains

$$\left|\frac{d\Delta}{dk_z}\right|_{k_z=k_z^{\pm}} \approx \frac{\Delta_S + \Delta_D}{2} d \approx \Delta_S d. \tag{87}$$

This gives

$$\mathcal{D}^{-1}_{va}(\mathbf{q},\Omega) = -iq\tau_0\frac{eB}{2\pi^2 g(\epsilon_F)} \equiv -iq\tau_0\Gamma, \tag{88}$$

i.e., an identical result to what we obtained before in the case of the Dirac metal.

The diagonal elements of the inverse diffusion propagator are also evaluated in exactly the same way as in the case of the Dirac metal. The form of the expression for the vector charge part of the propagator is, as before, constrained by the vector charge conservation:

$$\mathcal{D}^{-1}_{vv}(\mathbf{q},\Omega) = -i\Omega\tau_0 + Dq^2\tau_0, \tag{89}$$

where the diffusion coefficient is given by

$$D = \tilde{v}_F^2\tau_0\left\langle\frac{m_-^2(k_z)}{\epsilon_F^2}\right\rangle, \tag{90}$$

which is identical to the corresponding result in the Dirac metal case but with $\Delta(k_z)$ replaced by $m_-(k_z)$. The Fermi velocity in Eq. (90) is $\tilde{v}_F(k_z) = |d\Delta/dk_z|$, evaluated at the Weyl node locations, which is given by

$$\tilde{v}_F = \frac{d}{2b}\sqrt{\left(b^2 - b_{c1}^2\right)\left(b_{c2}^2 - b^2\right)}. \tag{91}$$

The average of $m_-^2(k_z)$ over the Fermi surface may be easily evaluated in the limit of small Fermi energy, which allows one to expand $m_-(k_z)$ to leading order in deviation of k_z from the Weyl node locations. In this case one obtains

$$D \approx \tfrac{1}{3}\tilde{v}_F^2\tau_0, \tag{92}$$

i.e., again identical to the corresponding Dirac metal result, obtained in Sec. III.

Finally, for the axial charge block of the inverse diffusion propagator we obtain the following expression:

$$\mathcal{D}^{-1}_{aa}(\mathbf{q},\Omega) = -i\Omega\tau_0 + \frac{\tau_0}{\tau_a} + Dq^2\tau_0, \tag{93}$$

where the axial charge relaxation rate is now given by

$$\frac{\tau_0}{\tau_a} = \frac{1 - (\tilde{v}_F/\Delta_S d)^2}{(\tilde{v}_F/\Delta_S d)^2}. \tag{94}$$

This expression for the axial charge relaxation rate represents the most significant difference of the Weyl metal case from the Dirac metal case. This equation shows, in particular, that in a Weyl metal the (dimensionless) axial charge relaxation rate is essentially always finite, even in the limit $\epsilon_F \to 0$. It may still be expected to be small, which is easily seen explicitly in the limit when $b_{c1} \ll b \ll b_{c2}$, and $\epsilon_F \ll b$. In this case we obtain

$$\frac{1}{\tau_a} \approx \frac{b^2}{4\Delta_S^2\tau_0}; \tag{95}$$

i.e., the axial charge relaxation increases quadratically with the spin-splitting parameter b as the Weyl nodes get split and separated out of the parent Dirac metal state. The diffusion equations themselves and the magnetoresistance formula are identical to the Dirac semimetal case, with the axial charge relaxation rate given by Eq. (95), so we will not repeat them explicitly here.

Before we conclude this section, we would like to point out an important caveat, which applies to the results of this section. Namely, all of the results above are only applicable if the condition

$$b_{c1} \ll b \ll b_{c2} \tag{96}$$

is satisfied. An implicit assumption here is that Weyl semimetal is obtained from a parent state, which is nearly a Dirac semimetal (hence the small $b_{c1} = |\Delta_S - \Delta_D|$), and we are far from the transition out of the Weyl semimetal state in the large-b limit, i.e., when $b = b_{c2}$. Only if the condition Eq. (96) is satisfied may we expect to get negative magnetoresistance, quadratic in the magnetic field in the general case. Otherwise, in magnetic Weyl semimetals, linear magnetoresistance, which is allowed by symmetry, will dominate the quadratic one at small fields. Under the condition Eq. (96), the linear terms in magnetoresistance are $O(b/b_{c2})$ and may thus be ignored. Linear magnetoresistance is strictly absent by symmetry, of course, in the case of noncentrosymmetric Weyl semimetals. In this case the above results apply without restriction.

V. DISCUSSION AND CONCLUSIONS

In this paper we have developed a theory of anomaly-related weak-field quadratic negative longitudinal magnetoresistance in Dirac and Weyl metals. An important issue is how to differentiate this novel magnetoresistance from other possible contributions, which are more mundane in origin. In fact, longitudinal magnetoresistance, which is what we are interested in here, in never entirely mundane. The reason is that, from the simplest Drude theory viewpoint, the only possible source of magnetoresistance is the Lorentz force, which is of course absent for electrons, propagating along the direction of the field. Drude theory thus predicts that longitudinal magnetoresistance is always absent, which is not the case: there are many examples of materials exhibiting it, even at low fields. Several possible sources of longitudinal magnetoresistance have been identified over the years [49–51], but perhaps the most universal source, related purely to the intrinsic properties of the electronic structure, was described recently by Pal and Maslov [52]. They have shown that longitudinal weak-field magnetoresistance arises necessarily when the shape of the Fermi surface exhibits certain types of angular anisotropy with respect to the direction of the magnetic field. This mechanism gives positive magnetoresistance, increasing quadratically with the magnetic field at low fields. For the anomaly-related negative magnetoresistance to be observable, it needs to be larger than this Fermi surface anisotropy–driven magnetoresistance. From this viewpoint, the Dirac metal case seems to be the best: one may expect both a weak anisotropy and a large axial relaxation time in this case. The Weyl metal case with either a very large separation between the nodes, i.e., separation approaching the size of the first BZ, or a very small separation (unless it arises from a parent zero-gap Dirac semimetal) is either way problematic, since the axial charge relaxation time may be expected to be small in these cases.

It is also important to remember that the theory presented in this paper applies only in the semiclassical limit, i.e., $\omega_B/\epsilon_F \ll 1$. In the opposite, ultraquantum limit, one may expect a linear negative magnetoresistance [35,36], which may be obtained from Eq. (72) by substituting the lowest LL density of states $g(\epsilon_F) \sim B$. It is also possible to have quadratic magnetoresistance of both signs in this limit, arising from the combined action of chiral anomaly and field-induced modification of the density of states [53]. One hopes that the current experiments [13,22,54–58] are in the semiclassical limit, as the quadratic magnetoresistance is observed at low fields, but the magnitude of the ratio ω_B/ϵ_F is at the moment uncertain in these experiments.

Finally, in the theory developed in the paper a particular model of the impurity scattering was assumed: weak pointlike Gaussian-distributed scatterers. This assumption was made primarily for computational convenience: the ladder sum for the diffusion propagator, Eq. (42), may only be calculated straightforwardly in this case, which is a limitation of the present approach. In many cases, a more physically realistic model should involve Coulomb impurities. In this case one might in fact expect that the axial relaxation rate should be even smaller, at least in the Weyl semimetal case, as the finite-momentum scattering, necessary to scatter electrons between the nodes, will be suppressed. However, a detailed calculation of this would certainly be helpful. What happens to the magnetoresistance in the strong-disorder limit [59–62] is also an important and experimentally relevant issue, worthy of a thorough study.

In conclusion, we have presented a theory of chiral-anomaly-driven negative quadratic longitudinal magnetoresistance in Dirac and Weyl metals in the weak magnetic field regime. We have demonstrated that this effect has two crucial ingredients. One is the coupling between the vector and the axial charge density, proportional to the magnetic field, which arises from the chiral lowest Landau level, or the nontrivial Berry curvature of the band eigenstates. This coupling will in principle exist in any system with a nonzero Berry curvature and is in this sense not specific to Dirac or Weyl metals, although the transport coefficient, describing such a coupling, has a universal value of $eB/2\pi^2$ in Dirac or Weyl metals only. The second ingredient is the near conservation of the axial charge density, manifesting in large axial charge relaxation time $\tau_a/\tau_0 \gg 1$. This property is specific to Dirac and Weyl metals only and is necessary for the negative quadratic magnetoresistance to be observable.

ACKNOWLEDGMENTS

Financial support was provided by Natural Sciences and Engineering Research Council (NSERC) of Canada.

[1] X. Wan, A. M. Turner, A. Vishwanath, and S. Y. Savrasov, Phys. Rev. B **83**, 205101 (2011).
[2] K.-Y. Yang, Y.-M. Lu, and Y. Ran, Phys. Rev. B **84**, 075129 (2011).
[3] A. A. Burkov and L. Balents, Phys. Rev. Lett. **107**, 127205 (2011).
[4] G. Xu, H. Weng, Z. Wang, X. Dai, and Z. Fang, Phys. Rev. Lett. **107**, 186806 (2011).
[5] S. M. Young, S. Zaheer, J. C. Y. Teo, C. L. Kane, E. J. Mele, and A. M. Rappe, Phys. Rev. Lett. **108**, 140405 (2012).
[6] Z. Wang, Y. Sun, X.-Q. Chen, C. Franchini, G. Xu, H. Weng, X. Dai, and Z. Fang, Phys. Rev. B **85**, 195320 (2012).

[7] Z. Wang, H. Weng, Q. Wu, X. Dai, and Z. Fang, Phys. Rev. B **88**, 125427 (2013).

[8] H. Weng, C. Fang, Z. Fang, B. A. Bernevig, and X. Dai, Phys. Rev. X **5**, 011029 (2015).

[9] S.-M. Huang, S.-Y. Xu, I. Belopolski, C.-C. Lee, G. Chang, B. Wang, N. Alidoust, G. Bian, M. Neupane, A. Bansil, H. Lin, and M. Zahid Hasan, Nat. Commun. **6**, 7373 (2015).

[10] S.-Y. Xu, I. Belopolski, N. Alidoust, M. Neupane, C. Zhang, R. Sankar, S.-M. Huang, C.-C. Lee, G. Chang, B. Wang, G. Bian, H. Zheng, D. S. Sanchez, F. Chou, H. Lin, S. Jia, and M. Zahid Hasan, arXiv:1502.03807.

[11] B. Q. Lv, H. M. Weng, B. B. Fu, X. P. Wang, H. Miao, J. Ma, P. Richard, X. C. Huang, L. X. Zhao, G. F. Chen, Z. Fang, X. Dai, T. Qian, and H. Ding, arXiv:1502.04684.

[12] S.-Y. Xu, C. Liu, S. K. Kushwaha, R. Sankar, J. W. Krizan, I. Belopolski, M. Neupane, G. Bian, N. Alidoust, T.-R. Chang, H.-T. Jeng, C.-Y. Huang, W.-F. Tsai, H. Lin, P. P. Shibayev, F.-C. Chou, R. J. Cava, and M. Zahid Hasan, Science **347**, 294 (2015).

[13] C. Zhang, S.-Y. Xu, I. Belopolski, Z. Yuan, Z. Lin, B. Tong, N. Alidoust, C.-C. Lee, S.-M. Huang, H. Lin, M. Neupane, D. S. Sanchez, H. Zheng, G. Bian, J. Wang, C. Zhang, T. Neupert, M. Zahid Hasan, and S. Jia, arXiv:1503.02630.

[14] L. Lu, Z. Wang, D. Ye, L. Ran, L. Fu, J. D. Joannopoulos, and M. Soljačić, arXiv:1502.03438.

[15] B. Q. Lv, N. Xu, H. M. Weng, J. Z. Ma, P. Richard, X. C. Huang, L. X. Zhao, G. F. Chen, C. Matt, F. Bisti, V. Strokov, J. Mesot, Z. Fang, X. Dai, T. Qian, M. Shi, and H. Ding, arXiv:1503.09188.

[16] S.-Y. Xu, N. Alidoust, I. Belopolski, C. Zhang, G. Bian, T.-R. Chang, H. Zheng, V. Strokov, D. S. Sanchez, G. Chang, Z. Yuan, D. Mou, Y. Wu, L. Huang, C.-C. Lee, S.-M. Huang, B. Wang, A. Bansil, H.-T. Jeng, T. Neupert, A. Kaminski, H. Lin, S. Jia, and M. Zahid Hasan, arXiv:1504.01350.

[17] S. Borisenko, Q. Gibson, D. Evtushinsky, V. Zabolotnyy, B. Büchner, and R. J. Cava, Phys. Rev. Lett. **113**, 027603 (2014).

[18] Z. K. Liu, B. Zhou, Y. Zhang, Z. J. Wang, H. M. Weng, D. Prabhakaran, S.-K. Mo, Z. X. Shen, Z. Fang, X. Dai, Z. Hussain, and Y. L. Chen, Science **343**, 864 (2014).

[19] M. Neupane, S.-Y. Xu, R. Sankar, N. Alidoust, G. Bian, C. Liu, I. Belopolski, T.-R. Chang, H.-T. Jeng, H. Lin, A. Bansil, F. Chou, and M. Z. Hasan, Nat. Commun. **5**, 5136 (2014).

[20] S.-Y. Xu, N. Alidoust, I. Belopolski, C. Zhang, G. Bian, T.-R. Chang, H. Zheng, V. Strokov, D. S. Sanchez, G. Chang, Z. Yuan, D. Mou, Y. Wu, L. Huang, C.-C. Lee, S.-M. Huang, B. Wang, A. Bansil, H.-T. Jeng, T. Neupert, A. Kaminski, H. Lin, S. Jia, and M. Zahid Hasan, arXiv:1504.01350.

[21] T. Sato, K. Segawa, K. Kosaka, S. Souma, K. Nakayama, K. Eto, T. Minami, Y. Ando, and T. Takahashi, Nat. Phys. **7**, 840 (2011).

[22] Q. Li, D. E. Kharzeev, C. Zhang, Y. Huang, I. Pletikosic, A. V. Fedorov, R. D. Zhong, J. A. Schneeloch, G. D. Gu, and T. Valla, arXiv:1412.6543.

[23] R. Y. Chen, S. J. Zhang, J. A. Schneeloch, C. Zhang, Q. Li, G. D. Gu, and N. L. Wang, arXiv:1505.00307.

[24] M. Z. Hasan and C. L. Kane, Rev. Mod. Phys. **82**, 3045 (2010).

[25] X.-L. Qi and S.-C. Zhang, Rev. Mod. Phys. **83**, 1057 (2011).

[26] G. Volovik, *The Universe in a Helium Droplet* (Clarendon, Oxford, 2003).

[27] G. E. Volovik, in *Quantum Analogues: From Phase Transitions to Black Holes and Cosmology*, Lecture Notes in Physics, Vol. 718, edited by W. Unruh and R. Schtzhold (Springer, Berlin, 2007).

[28] M. Kohmoto, B. I. Halperin, and Y.-S. Wu, Phys. Rev. B **45**, 13488 (1992).

[29] A. A. Zyuzin and A. A. Burkov, Phys. Rev. B **86**, 115133 (2012).

[30] S. T. Ramamurthy and T. L. Hughes, arXiv:1405.7377.

[31] F. R. Klinkhamer and G. E. Volovik, Int. J. Mod. Phys. A **20**, 2795 (2005).

[32] K. Fukushima, D. E. Kharzeev, and H. J. Warringa, Phys. Rev. D **78**, 074033 (2008).

[33] S. L. Adler, Phys. Rev. **177**, 2426 (1969).

[34] J. S. Bell and R. Jackiw, Nuovo Cimento A **60**, 4 (1969).

[35] H. Nielsen and M. Ninomiya, Phys. Lett. B **130**, 389 (1983).

[36] V. Aji, Phys. Rev. B **85**, 241101 (2012).

[37] P. Hosur, S. Ryu, and A. Vishwanath, Phys. Rev. B **81**, 045120 (2010).

[38] S. Ryu, J. E. Moore, and A. W. W. Ludwig, Phys. Rev. B **85**, 045104 (2012).

[39] A. Furusaki, N. Nagaosa, K. Nomura, S. Ryu, and T. Takayanagi, C. R. Phys. **14**, 871 (2013).

[40] A. A. Zyuzin, S. Wu, and A. A. Burkov, Phys. Rev. B **85**, 165110 (2012).

[41] M. M. Vazifeh and M. Franz, Phys. Rev. Lett. **111**, 027201 (2013).

[42] Y. Chen, S. Wu, and A. A. Burkov, Phys. Rev. B **88**, 125105 (2013).

[43] D. T. Son and B. Z. Spivak, Phys. Rev. B **88**, 104412 (2013).

[44] A. A. Burkov, Phys. Rev. Lett. **113**, 247203 (2014).

[45] A. A. Burkov, J. Phys.: Condens. Matter **27**, 113201 (2015).

[46] A. A. Burkov, M. D. Hook, and L. Balents, Phys. Rev. B **84**, 235126 (2011).

[47] A. Altland and B. D. Simons, *Condensed Matter Field Theory*, 2nd ed. (Cambridge University Press, New York, 2010).

[48] A. A. Burkov, Phys. Rev. Lett. **113**, 187202 (2014).

[49] E. H. Sondheimer, Proc. R. Soc. London A **268**, 100 (1962).

[50] D. Stroud and F. P. Pan, Phys. Rev. B **13**, 1434 (1976).

[51] D. L. Miller and B. Laikhtman, Phys. Rev. B **54**, 10669 (1996).

[52] H. K. Pal and D. L. Maslov, Phys. Rev. B **81**, 214438 (2010).

[53] P. Goswami, J. H. Pixley, and S. Das Sarma, arXiv:1503.02069.

[54] J. Xiong, S. Kushwaha, J. Krizan, T. Liang, R. J. Cava, and N. P. Ong, arXiv:1502.06266.

[55] J. Xiong, S. K. Kushwaha, T. Liang, J. W. Krizan, W. Wang, R. J. Cava, and N. P. Ong, arXiv:1503.08179.

[56] X. Huang, L. Zhao, Y. Long, P. Wang, D. Chen, Z. Yang, H. Liang, M. Xue, H. Weng, Z. Fang, X. Dai, and G. Chen, arXiv:1503.01304.

[57] C.-Z. Li, L.-X. Wang, H. Liu, J. Wang, Z.-M. Liao, and D.-P. Yu, arXiv:1504.07398.

[58] C. Zhang, E. Zhang, Y. Liu, Z.-G. Chen, S. Liang, J. Cao, X. Yuan, L. Tang, Q. Li, T. Gu, Y. Wu, J. Zou, and F. Xiu, arXiv:1504.07698.

[59] B. Sbierski, G. Pohl, E. J. Bergholtz, and P. W. Brouwer, Phys. Rev. Lett. **113**, 026602 (2014).

[60] S. V. Syzranov, L. Radzihovsky, and V. Gurarie, Phys. Rev. Lett. **114**, 166601 (2015).

[61] S. V. Syzranov, V. Gurarie, and L. Radzihovsky, Phys. Rev. B **91**, 035133 (2015).

[62] B. Sbierski, E. J. Bergholtz, and P. W. Brouwer, arXiv:1505.07374.